

CO₂ capture performance of calcium-based synthetic sorbent with hollow core-shell structure under calcium looping conditions

Xiaotong Ma^a, Yingjie Li^{a*}, Lunbo Duan^b, Edward Anthony^c, Hantao Liu^d

^a School of Energy and Power Engineering, Shandong University, Jinan 250061, China

^b Key Laboratory of Energy Thermal Conversion and Control of Ministry of Education, Southeast
University, Nanjing 210096, China

^c Centre for Combustion and CCS, Cranfield University, Cranfield, Bedfordshire MK43 0AL, UK

^d School of Energy and Power Engineering, North University of China, Taiyuan 030051, China

Abstract

A novel calcium-based synthetic CO₂ sorbent with hollow core-shell structure was prepared by a carbon microsphere template route where carbide slag, alumina cement and glucose were employed as the low-cost calcium precursor, support and carbon source, respectively. The effects of the alumina cement addition, the pre-calcination temperature during the preparation process, the carbon template addition and calcination conditions on CO₂ capture performances of the calcium-based synthetic sorbents were studied during calcium looping cycles. The synthetic sorbent containing 5 wt.% alumina cement possesses the highest CO₂ capture capacity during calcium looping cycles, which is mainly composed of CaO and Ca₁₂Al₁₄O₃₃. The CO₂ capture capacities of the synthetic sorbent under mild and severe calcination conditions can retain 0.37 and 0.29 g/g after 20 cycles, which are 57% and 99% higher than those of carbide slag under the same conditions, respectively.

* Corresponding author: Tel.: +86-531-88392414; E-mail: liyj@sdu.edu.cn (Y. Li).

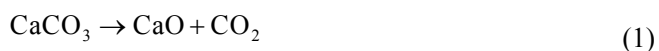
The synthetic sorbent possesses a hollow micro-sphere morphology with a nano-structured shell and meso-porous structure, which decreases the diffusion resistance of CO₂. Periodic density functional theory (DFT) calculations are used to explain why Ca₁₂Al₁₄O₃₃ can effectively retard both agglomeration and sintering of the synthetic sorbent. The hollow core-shell model is proposed to explain the CO₂ capture mechanism of the synthetic sorbent. For the same CO₂ capture efficiency, the energy consumption in the calciner using the synthetic sorbent is much lower than that using carbide slag and natural limestone. This work designs a good method to prepare the hollow sphere-structured synthetic sorbents with high CO₂ capture capacity and provides a promising way to integrate efficient CO₂ capture with the utilization of industrial waste.

Key words: Carbide slag; Carbon template; Hydrothermal carbonization; Calcium looping; CO₂ capture

1. Introduction

The increasing concentration of greenhouse gases, especially CO₂, in the atmosphere is clearly likely linked to climate change [1,2]. Therefore, the reduction of CO₂ emission has received increasing attention due to concerns over environmental protection [3-6]. The calcium looping (CaL) process provides an alternative and potentially efficient strategy for CO₂ capture for power generation from fossil fuels and hydrogen production with in-situ CO₂ capture [7,8]. The CaL process typically utilizes calcium-based sorbents to transform low concentrations of CO₂ from flue gas into concentrated CO₂, resulting in effective Carbon Capture, Utilization and Storage (CCUS). The overall process involves cyclic calcination and carbonation reactions of the calcium-based

sorbent, as respectively shown in Eqs. (1) and (2).



The CO₂ capture capacity and cyclic stability of the calcium-based sorbents are the critical considerations for the CaL process. An ideal sorbent should possess the ability to both absorb significant amounts of CO₂ and to be resistant to repeated thermal and mechanical shocks. The CO₂ capture capacity of calcium-based sorbent decreases rapidly with the number of calcination/carbonation cycles due to sintering [9,10]. This problem brings about the discharge of deactivated sorbents and the addition of a great quantity of fresh sorbents in the calciner to maintain the overall CO₂ capture efficiency at a high level, which results in a significant increase in the energy consumption in the calciner [10]. Li et al. [11] found that 49 kJ energy (per mole of CO₂ entering the carbonator) can be saved for the CO₂ capture efficiency of 0.95 when modified limestone with acetic acid solution instead of limestone is used under the mild calcination condition. Lowering the calcination temperature, e.g., adoption of high-concentration steam rather than high-concentration CO₂ as the calcination atmosphere, improves the CO₂ capture efficiency from 0.68 to 0.88 and reduces energy consumption in the calciner by 25% [12]. Thus, the energy consumption in the calciner apparently decreases with the increased cyclic CO₂ capture capacity of the calcium-based sorbents. Therefore, it is of practical importance to improve CO₂ capture performance of calcium-based sorbents during the calcium looping process.

Numerous research studies have focused on how to improve the CO₂ capture performance of calcium-based sorbent. Methods including the modification of microstructure and improvement in sintering resistance of calcium-based sorbent are effective. Antzara et al. [13] found that the type of

combustion agent used in the sol-gel auto-combustion route influenced dramatically the initial CO₂ sorption capacity of the prepared sorbent and the use of citric acid resulted in the sorbent with the highest surface area and initial sorption capacity. Blamey et al. [14] suggested that periodic reactivation by hydration is a feasible way for the enhancement of sorbents and the degree of hydration was linked to the subsequent carbonation level. Valverde et al. [15] investigated sorbents pre-calcined under CO₂ at high temperatures. A drastic reduction of the CaO reactive surface area and the formation of macropores were observed as a result of enhanced sintering during pretreatment. Despite the low initial activity, reactivation was observed in the following cycles. Chen et al. [16] prepared CaO-MgO and CaO-MnO₂ by the sol-gel method. The two sorbents achieved carbonation conversions of 79% and 76%, respectively, after 50 cycles. Jing et al. [9] produced CaO/Ca₃Al₂O₆ sorbent and demonstrated that the sorbent with CaO to Al₂O₃ mass ratio of 8:2 displayed a carbonation conversion of about 52%, comparing to 12% for the pure CaO sorbent. Benitez-Guerrero et al. [17] found that Ca₄Al₆O₁₃ (Ca/Al<1) was formed under calcium looping conditions by milling mixtures of nanoalumina and natural limestone powders, which helped stabilize the CaO microstructure and mitigated pore-plugging.

Carbon templating is a promising way to synthesize ordered mesoporous materials due to its advantage in improving surface area and providing good prospects for gas adsorption [18,19], catalysis [20], energy storage and conversion [18,21], etc. Recently, carbon templating has been exploited in applications to overcome the loss-in-capacity problem of calcium-based CO₂ sorbent. Three synthesis methods using carbon template have been reported and tested with varying degrees of success: (i) pyrolysis of organometallic calcium precursors, (ii) acidification with organic acid, and (iii) the utilization of chemical reaction, such as poly-condensation. After pyrolysis in an inert

atmosphere, in-situ carbon was formed from organometallic matter, which appears to serve as a template for controlling the structure of the sorbent. Wang et al. [22] used citric acid as a carbon source to produce the coated carbon, which effectively prevented the separation of CaO and MgO in dolomite, such that its initial carbonation conversion of 92% only decreased to 54% after 20 cycles. Zhao et al. [23] employed the carbon template method to modify the microstructure of calcined organometallic calcium compounds (e.g., calcium acetate, calcium citrate, and calcium gluconate) for high-temperature CO₂ capture and they found that calcium gluconate showed the highest CO₂ capture uptake of 0.52 g/g after 10 cycles. However, the major problem related to these techniques is that the micro-morphology of the sorbent, which strongly impacts the CO₂ capture performance, cannot be controlled easily. Exploring a general strategy to tailor the structure of the sorbent is of scientific and technological importance due to the current unpredictability of the various approaches. Broda et al. [24] prepared carbon gel templated, Ca-rich, Al₂O₃-stabilized CO₂ sorbents by poly-condensation of resorcinol with formaldehyde. A hollow microsphere with a nano-structured shell was obtained after the removal of the carbon gel template. Although the average diameter and probable morphology of sorbent could be predicted, the carbon template material, formaldehyde, was environmentally unfriendly.

Large quantities of high-calcium solid wastes are generated during some major industrial operations every year. Among them, carbide slag, as a by-product from the hydrolysis process of calcium carbide (CaC₂) for ethyne production, is landfilled, which represents the waste of calcium sources. An interesting possibility is to utilize carbide slag as a candidate for CO₂ capture [25]. The CO₂ capture performance of carbide slag can be further improved by adding supports such as Al₂O₃ [26], MgO [27], cement [28,29], etc. However, the critical flaw of the above method is that the

structure of the obtained modified carbide slag cannot be controlled. The control of the microstructure and the regulation of the components are beneficial for the determination in the CO₂ capture capacity and the cyclic stability of the calcium-based sorbent during the multiple calcination/carbonation cycles.

Hydrothermal carbonization (HTC), i.e., aqueous carbonization at elevated temperature and pressure, has recently been suggested as an efficient chemical process for the conversion of biomass to structured carbons, offering a new way to produce nano/micro-structured carbon [30,31]. In this work, we used the micro-structured carbon produced by HTC of glucose as a carbon template to fabricate a novel synthetic sorbent from carbide slag and alumina cement. The synthetic sorbent obtained, possessed a hollow core-shell structure, high CO₂ capture capacity and good sintering resistance. Thus, this work provides a novel method to synthesize an efficient calcium-based synthetic sorbent for calcium looping, where the microstructure and the compositions of the sorbent can be controlled and regulated. Low-cost, environmental friendly materials make this method more feasible and practical. The effects of alumina cement addition, pre-calcination temperature during the preparation process, carbon template addition and calcination conditions on CO₂ capture performance of the synthetic sorbent were studied under mild and severe calcination conditions. The CO₂ capture mechanisms and the sintering resistance of the synthetic sorbents were revealed by the microstructure analysis and periodic density functional theory (DFT) calculations. Moreover, the energy consumptions in the calciner using carbide slag and synthetic sorbents were calculated and compared.

2. Experimental

2.1. Materials

The carbide slag was sampled from a chlor-alkali plant in Shandong Province, China. The alumina cement was obtained from a cement plant in Jinan, Shandong Province, China. The chemical components of the carbide slag and the alumina cement are shown in Table 1. Analytical-grade glucose was used as the carbon source and deionized water was the solvent.

2.2 Preparation of calcium-based synthetic sorbent

The calcium-based synthetic sorbents were prepared by HTC of glucose. First, glucose was dissolved in 60 mL deionized water (0.1-1 mol/L). After complete dissolution, 5 g carbide slag and 0%, 5% or 15% of alumina cement were added to the aqueous solution, respectively. The suspension was stirred in a water bath at 60 °C for 30 min. The resulting slurry was put into a high-pressure kettle for hydrothermal synthesis at 180 °C for 6 h. After cooling to room temperature, a dark brown solid precipitate was collected, washed with water and ethanol, and then dried. Pyrolysis of the obtained precipitate was carried out in a tubular furnace under a nitrogen flow of 0.5 L/min at a heating rate of 3 °C/min followed by maintenance at 450 °C for 2 h. Finally, the material obtained was pre-calcined under air at 400-800 °C for 1 h in a muffle furnace. Two synthetic sorbents with alumina cement contents of 5% and 15% were obtained, respectively. The same preparation process was also performed without the addition of alumina cement. Additionally, a synthetic sorbent sample with alumina cement content of 5% was obtained by the normal wet-mixing method, as a comparison to the synthetic sorbent prepared by the carbon microsphere-template method. Weighed amounts of carbide slag and alumina cement were mixed in a glass beaker. Water was added with stirring and the gel obtained was then air-dried for 24 h. All the sorbents were labeled using codes.

CMT and WM denote carbon microsphere-templated and wet-mixing methods, respectively. Figures in the sorbent composition descriptions denote the different weight percentages of alumina cement in the synthetic sorbents. For example, CMT-5 denotes the synthetic sorbent with 5 wt.% alumina cement by carbon microsphere-templated method.

2.3. Cyclic CO₂ capture test

The CO₂ capture experiments were performed in a dual fixed-bed reactor (DFBR) including a carbonator and a calciner, as illustrated in Fig. 1. Typically, 200 mg of the sample was loaded in the calciner under the mild calcination condition (pure N₂ at 850 °C) for 10 min or the severe calcination condition (70% CO₂/N₂ at 920 °C) for 10 min. The gas mixture was supplied at a flow rate of 1 L/min to the calciner. Following this step, the calcined sample was taken out from the calciner and then placed in the carbonator at 700 °C under 15% CO₂ (N₂ balance) for 20 min, thereby completing the carbonation process. The repetitive tests were performed to simulate the multiple calcination/carbonation cycles of the samples for CO₂ capture. The samples were taken out from the calciner and the carbonator and the mass changes of the samples during the cycles were measured by a delicate Mettler Toledo-XS105DU electronic balance (with the accuracy of 0.1 mg). The CO₂ capture capacity and carbonation conversion were used to evaluate the CO₂ capture performance of the samples, as follows:

$$C_N = \frac{m_N - m_{\text{cal},N}}{m_0} \quad (3)$$

$$X_N = \frac{m_N - m_{\text{cal},N}}{m_0 \cdot b} \cdot \frac{M_{\text{CaO}}}{M_{\text{CO}_2}} \quad (4)$$

2.4. Characterization

A D/Max- \square A X-ray diffraction (XRD) instrument was used to characterize the phase

compositions of the synthetic sorbent. A Micromeritics ASAP 2020-M nitrogen adsorption analyzer was used to evaluate pore structure characteristics of the synthetic sorbent. The surface area and pore volume of the synthetic sorbent were calculated in terms of the BET (Brunauer-Emmett-Teller) method and BJH (Barrett-Joyner-Halenda) model, respectively. A SUPRATM 55 field emission scanning electron microscope (SEM) was used to detect micro-morphologies of the pure carbon template after hydrothermal processing of 6 h and the synthetic sorbents with different hydrothermal durations (3, 6 and 12 h) in order to monitor the evolution of hydrothermal carbonation.

2.5. Computational model and method

Calculations were performed using the DFT method, for which the nonlocal generalized gradient approximation (GGA) and the Perdew-Wang 1991 (PW91) function in CASTEP (Cambridge Serial Total Energy Package) was chosen. An ultra-soft pseudopotential was used to deal with the interaction between ion cores and valence electrons. The energy cutoff was chosen to be 600 eV and the k-points separation was selected to be 0.06 \AA^{-1} . The Broyden-Fletcher-Goldfarb-Shanno (BFGS) scheme was employed as the minimization algorithm.

3. Results and Discussion

3.1. XRD analysis

Fig. 2 shows the XRD spectrum of CMT-5. It is found that the main compositions of CMT-5 are CaO and $\text{Ca}_{12}\text{Al}_{14}\text{O}_{33}$, with a small amount of $\text{Ca}_2\text{Al}_2\text{SiO}_7$. This result supports the theory that the chemical interaction between CaO and alumina cement results in the formation of $\text{Ca}_{12}\text{Al}_{14}\text{O}_{33}$. $\text{Ca}_{12}\text{Al}_{14}\text{O}_{33}$ is an effective inert support to weaken the agglomeration degree of CaO/ CaCO_3 particles [32-34]. This explains the better cyclic stability of the synthetic sorbent than carbide slag during CO_2 capture cycles.

3.2. Effect of alumina cement addition on CO₂ capture by synthetic sorbents

Fig. 3 shows the CO₂ capture capacities of carbide slag and synthetic sorbents. Different degrees of activity loss for all of the sorbents with the number of cycles are observed, which is believed to be caused by the sintering. Carbide slag shows the highest C_1 of 0.58 g/g, but C_{10} drops to 0.3 g/g. WM-5 shows a similar decay trend as that of carbide slag, while C_N for CMT-5 remains stable during repetitive cycles. This suggests that alumina cement has a stronger effect on improving the sintering-resistance behavior of CaO particles when the carbon-templated method instead of wet mixing method is employed. Despite the lower C_1 of 0.44 g/g and 0.40 g/g for CMT-5 and CMT-15, C_{10} retain 0.39 g/g and 0.34 g/g representing decay of about 11% and 14%, respectively. This work demonstrates that the synthetic sorbents possess better cyclic stability than carbide slag. C_{10} was higher for CMT-0 than for carbide slag. This is possibly due to the formation of C-S-H (hydrated calcium silicate) in the hydrothermal reaction between Ca(OH)₂ and SiO₂ existing in carbide slag. Interestingly, this reaction is also a promising route for the production of porous ceramics [7]. Shi et al. [35] found that C-S-H contributed to better CO₂ capture of the CaO/sepiolite sorbent. However, the evidence for significant changes in the material could not be detected by XRD analysis, due to the limited content of C-S-H. It is found that CMT-5 achieves the highest C_{10} , 0.39 g/g, which is 1.3 times as high as that of carbide slag and 2 times as high as that of the natural limestone reported by Grasa and Abanades [36]. Increasing the amount of alumina cement decreases the C_1 of CMT-15, which may be attributed to the decreased active CaO content in the synthetic sorbent. Therefore, the subsequent research has been concentrated on CMT-5.

3.3. Effect of pre-calcination temperature during preparation on CO₂ capture by synthetic sorbents

Fig. 4 presents the CO₂ capture capacities of the synthetic sorbents at different pre-calcination

temperatures during the preparation process. The pre-calcination temperature (examined at 100 °C intervals between 400 and 800 °C) shows a slight effect on the CO₂ capture capacities of the synthetic sorbents. C_N increases with increasing the pre-calcination temperature from 400 to 600 °C, while it decreases with increasing the temperature further. Higher pre-calcination temperature leads to a higher solid-state reaction rate for the generation of Ca₁₂Al₁₄O₃₃, but it also intensifies the sintering of the synthetic sorbents, which leads to poorer CO₂ capture performance [37]. Therefore, the optimum pre-calcination temperature is 600 °C, which is adopted in the following experiments.

3.4. Effect of carbon template addition on CO₂ capture by synthetic sorbents

To further confirm the optimal amount of carbon template, CO₂ capture capacities of the synthetic sorbents with different amounts of glucose during the preparation process were studied and the results are presented in Fig. 5. Increasing the concentration of glucose solution in the range of 0.5-1 mol/L improves the effectiveness of the carbon template on the enhancement in CO₂ capture by the synthetic sorbents. The results show that the best performance tested was found at 1 mol/L, and C_{10} of CMT-5 with 1 mol/L of glucose is 12% and 37% higher than those with 0.5 and 0.1 mol/L, respectively. The reason for the higher CO₂ capture capacity due to the increased concentration of glucose solution might be the effective load of carbide slag on the carbon template during the hydrothermal reaction. For instance, the CO₂ capture performance of the synthetic sorbent with 0.1 mol/L glucose is no different than that for carbide slag alone. Only a small portion of carbide slag is loaded because of the very small amount of carbon formed when the glucose concentration is 0.1 mol/L. Therefore, to obtain stable CO₂ capture performance of the synthetic sorbents, 1 mol/L of glucose is relatively economic and a reasonable choice.

3.5. Effect of calcination conditions on CO₂ capture by synthetic sorbent

In the industrial application, the calcination of the calcium-based sorbent occurs under high concentration of CO_2 , in which case, the calcination temperature needs to be raised for the complete decomposition of CaCO_3 and cyclic utilization of CaO . However, the high calcination temperature leads to the block and collapse of pores in the generated CaO due to the severe sintering [36]. Thus, the study on CO_2 capture by synthetic sorbents under the severe calcination conditions (high CO_2 concentration and high temperature above $900\text{ }^\circ\text{C}$) is important. Multi-cyclic CO_2 capture capacities of CMT-5 and carbide slag under the mild calcination conditions (pure N_2 and $850\text{ }^\circ\text{C}$) and the severe calcination conditions ($70\%\text{ CO}_2/\text{N}_2$ and $920\text{ }^\circ\text{C}$) are plotted in Fig. 6. Both CMT-5 and carbide slag under the severe calcination conditions show lower CO_2 capture capacities for 20 cycles, compared to those seen under the mild calcination conditions, which means as expected that the severe calcination conditions do have an adverse impact on CO_2 capture behavior of the sorbent. Under the severe calcination condition, C_{20} of carbide slag is around 0.11 g/g , while C_{20} of CMT-5 is about 0.21 g/g . C_{20} of CMT-5 under the mild and the severe calcination conditions are almost 1.6 and 2 times as high as those of carbide slag, respectively. Deactivation of CMT-5 with respect to CO_2 capture capacity is mitigated due to the formation of $\text{Ca}_{12}\text{Al}_{14}\text{O}_{33}$, which can effectively hinder the agglomeration and aggregation of CaO particles. Thus, the carbon microsphere-templated synthetic sorbent is better for CO_2 capture under the severe calcination conditions.

3.6. Simulation calculations on the interactions between support and CaO in synthetic sorbents

The CaO unit cell adopts a cubic structure (225 Fm-3m space group) and the $\text{Ca}_{12}\text{Al}_{14}\text{O}_{33}$ unit cell adopts a cubic structure (220 I-43d space group), as shown in Fig. 7(a) and (b), respectively. To simulate the active phase for CO_2 capture that adheres to the support, a cubic Ca_4O_4 nanocluster is built because it reflects the structural features of a real CaO cluster and can reduce the computational

consumption. The CaO cluster is optimized in a cubic box of $20 \text{ \AA} \times 20 \text{ \AA} \times 20 \text{ \AA}$ to eliminate the periodicity effects. For the CaO and $\text{Ca}_{12}\text{Al}_{14}\text{O}_{33}$ bulk calculations, the k-point sampling scheme of the Monkhorst-Pack grid of $6 \times 6 \times 6$ is chosen. All the unit cell optimization is regarded as converged when the atomic forces, maximum displacement, the stress on the atoms and total energy variation are less than 0.03 eV/\AA , $1 \times 10^{-3} \text{ \AA}$, 0.05 GPa , and $1 \times 10^{-5} \text{ eV/atom}$, respectively. The lattice parameters of geometric structures after the optimization are shown in Table 2.

The CaO (1 0 0) surface is used to study the CO_2 capture characteristics of CaO, since this surface is the most stable low-index CaO surface, as discussed by Tao et al. [40] and Galloway et al. [41]. $\text{Ca}_{12}\text{Al}_{14}\text{O}_{33}$ (1 1 0) is selected because the (1 1 0) surface is recognized as the most close-packed plane in the crystals with the body-centered cubic structure [42]. The CaO (1 0 0) surface and $\text{Ca}_{12}\text{Al}_{14}\text{O}_{33}$ (1 1 0) surfaces are cleaved from the CaO and $\text{Ca}_{12}\text{Al}_{14}\text{O}_{33}$ unit cell. CaO (1 0 0) with a (2×2) periodic supercell and $\text{Ca}_{12}\text{Al}_{14}\text{O}_{33}$ (1 1 0) slabs with a (1×1) periodic cell are constructed, as shown in Fig. 8(a) and (b), respectively. The CaO cluster and upper several layers (3 layers for CaO and 6 layers for $\text{Ca}_{12}\text{Al}_{14}\text{O}_{33}$) are allowed to be fully relaxed, whereas the bottom layers are kept frozen in their bulk positions, which is sufficient to describe the substrate property. A vacuum layer of 20 \AA is used to prevent interaction between the periodic slabs.

For the adsorption of the CaO cluster on the CaO (1 0 0) and $\text{Ca}_{12}\text{Al}_{14}\text{O}_{33}$ (1 1 0) surfaces, the adsorption energy E_{ad} is defined as

$$E_{\text{ad}} = (E_{\text{sur}} + E_{\text{Ca}_4\text{O}_4}) - E_{\text{Ca}_4\text{O}_4/\text{sur}} \quad (5)$$

where E_{sur} and $E_{\text{Ca}_4\text{O}_4}$ are the total energies of the CaO (1 0 0) or $\text{Ca}_{12}\text{Al}_{14}\text{O}_{33}$ (1 1 0) surface and the free CaO cluster; $E_{\text{Ca}_4\text{O}_4/\text{sur}}$ is the total system energy of the CaO cluster supported on the surface. A positive E_{ad} indicates that the system is more stable than the separated cluster and surface and a

higher value of E_{ad} represents a stronger affinity towards the CaO cluster and surface.

Previous studies have shown that $\text{Ca}_{12}\text{Al}_{14}\text{O}_{33}$ can stabilize the CO_2 capture activities of sorbents, which is attributed to its high melting point and physical separation between CaO/CaCO_3 particles [32, 43]. Liu et al. [44] built a model of CaO (1 0 0) surface promoted by Al, in which one surface-layer Ca atom was substituted by one Al atom. The results demonstrate the strong bonding interaction between O atoms from CaO cluster and the Al site of the promoted CaO (1 0 0) surface, which inhibited the migration and growth of CaO particles. However, the simplified model cannot reflect the structural features of the real structure of $\text{Ca}_{12}\text{Al}_{14}\text{O}_{33}$, as the underlying mechanisms of sintering inhibition have not been comprehensively studied. Therefore, the CaO cluster supported on real $\text{Ca}_{12}\text{Al}_{14}\text{O}_{33}$ (1 1 0) surface is used here. The calculation using the same CaO cluster supported on CaO (1 0 0) surface is also performed as a comparison.

The optimized CaO cluster is added to the $\text{Ca}_{12}\text{Al}_{14}\text{O}_{33}$ (1 1 0) and CaO (1 0 0) surfaces and the systems are optimized. The most stable states of these two systems are shown in Fig. 9(a) and (b), respectively. For the optimized structure of CaO cluster supported on $\text{Ca}_{12}\text{Al}_{14}\text{O}_{33}$ (1 1 0) surface, 7 bonds are newly formed. Ca atoms from the cluster only form bonds with surface O atoms, while O atoms from the cluster form bonds with both surface Ca and Al atoms. The bond characteristics are simple in the model containing CaO surface. Two new bonds between Ca and O atoms are formed. The bond lengths are given in Table 3. The bond lengths of $\text{Ca}^c\text{-O}^s$ and $\text{O}^c\text{-Ca}^s$ in the model containing $\text{Ca}_{12}\text{Al}_{14}\text{O}_{33}$ surface are about the same as those of the model containing CaO surface. The bond lengths of $\text{O}^c\text{-Al}^s$ in the model containing $\text{Ca}_{12}\text{Al}_{14}\text{O}_{33}$ surface are much shorter than any other bonds. This suggests that Al sites on the $\text{Ca}_{12}\text{Al}_{14}\text{O}_{33}$ surface have strong affinities with the cluster, which play important parts in the interaction between CaO and $\text{Ca}_{12}\text{Al}_{14}\text{O}_{33}$ surface. The

adsorption energies of the two models are calculated and the results are given in Table 4. Compared with CaO surface, $\text{Ca}_{12}\text{Al}_{14}\text{O}_{33}$ as a support results in higher adsorption energy, which is 2.34 times as high as that of the system with CaO cluster and CaO surface. This indicates that the stability of the synthetic sorbents with this system would be enhanced because the mobility of CaO cluster is reduced with increased binding force. It is interesting to find that the structure of the cluster seems to be disordered in the structure of CaO cluster supported on CaO (1 0 0) surface but it keeps its original state in the model containing $\text{Ca}_{12}\text{Al}_{14}\text{O}_{33}$, as shown in Fig. 9(a) and (b). The stable skeleton contributes to the better sintering resistance of the synthetic sorbents, a fact which is also supported by previous experimental results.

3.7. Microstructure analysis

Fig. 10 shows SEM images of the typical structural patterns of pure carbon template and CMT-5 after the different preparation steps. Remarkably, the pure carbon template possesses monodisperse spheres with smooth outer surface, as shown in Fig. 10(a). This form provides a possible loading base for manufacturing the synthetic sorbents with core-shell structure. The average diameter of the carbon spheres is around 3 μm . By comparison of Fig. 10(b), (c) and (d), the morphologies of CMT-5 with different hydrothermal intervals appear different. 3h of hydrothermal interval only leads to the formation of shapeless and interconnected stacking carbon spheres. Well-shaped carbon spheres are formed with the hydrothermal interval of 6 h. With the hydrothermal carbonation proceeding from 3 to 12 h, the spheres grow on average from 2 to 10 μm in size. Apparently, the outer covering becomes rough after carbide slag and alumina cement are loaded around the carbon template, as illustrated in Fig. 10 (c) and (d). After calcination under air at 600 °C for 1 h, the carbon template is removed in CMT-5, leaving a hollow sphere with a cage-like shell, as shown in Fig. 10(e). Fig.

10(f) shows a magnified view of the shell. It can be observed that the cage-like shell possesses a porous surface. The porous structure may further decrease the diffusion resistance of CO₂ in the synthetic sorbent, which is beneficial for CO₂ capture.

The pore characteristics were analyzed in more detail by N₂ adsorption. As shown in Table 5, the surface area and pore volume of CMT-5 are higher than those of calcined carbide slag. The same conclusion can be drawn after 10 cycles, i.e., the surface area and pore volume of CMT-5 are 2.6 and 3.6 times higher than those of carbide slag. The better pore characteristics favor the better contact between CaO particles in CMT-5 and CO₂, which leads to the higher carbonation degree. N₂ adsorption-desorption isotherms of CMT-5 are presented in Fig. 11(a). It is found that CMT-5 possesses a typical mesoporous structure. This mesoporous structure is precisely composed of pores in the range of 10-100 nm in diameter, as shown in Fig. 11(b). Moreover, the mesopores in CMT-5 are maintained to a greater degree and the cumulative volume of pores in the range of 10-100 nm in diameter is up to 2.7 times as high as that of carbide slag. The pores in the range of 10-100 nm in diameter have been proved to play a major role in CO₂ capture by calcium-based sorbents [29], which indicates that the pore size distribution of CMT-5 is more favorable for carbonation. Thus, CMT-5 can achieve higher CO₂ capture capacity than carbide slag over multiple cycles.

A possible explanation based on a hollow core-shell model is proposed, as shown in Fig. 12. When depicted like the conventional solid sphere model, CaO can achieve complete carbonation in the first cycle. However, the progressive deactivation occurs in the following cycles due to sintering of the sorbent especially during the calcination step [45], with the residual capacity rapidly decreasing to 0.14 g/g after 10 cycles. The diffusion resistance of CO₂ increases because of the thicker CaCO₃ product layer, resulting in partial carbonation in the following cycles. Therefore, the carbonation

degree decreases and the unreacted CaO core grows with the number of cycles. The major difference between the hollow core-shell model and conventional solid sphere model is that the hollow core-shell structure increases the exposed surface area of the synthetic sorbent, which avoids the growth of unreacted CaO core to the greatest extent. Moreover, the physical separation effects of the inert materials, e.g., $\text{Ca}_{12}\text{Al}_{14}\text{O}_{33}$, further stabilize the cyclic CO_2 capture reactivity of CaO, which is attributed to the superior CO_2 capture performance of the synthetic sorbent tested in this work.

3.8. Analysis of energy consumption in calciner

Energy consumption values in the calciner using carbide slag, CMT-5 and limestone during cycles are calculated and compared. The energy consumption in the calciner for capturing one mole of CO_2 [12] is selected for its simplicity and accuracy in this work. The physical parameters are listed in Table 6. In order to simplify the calculation process, the same calcination/carbonation condition is applied in all calculations with carbide slag, CMT-5 and limestone. Assuming that sorbents are continuously fed in the system and the fresh sorbents can be mixed well with the previous sorbents, the energy consumption for capturing one mole of CO_2 can be described by Eq. (6) [12].

$$\frac{H_{\text{cal}}}{E_{\text{CO}_2} F_{\text{CO}_2}} = \frac{F_{\text{R}}}{E_{\text{CO}_2} F_{\text{CO}_2}} \left\{ \int_{T_{\text{car}}}^{T_{\text{cal}}} [c_{p,\text{CaO}}(1 - X_{\text{ave}}) + c_{p,\text{CaCO}_3} X_{\text{ave}} + c_{p,\text{inert}} F_{\text{R,inert}}] dT \right. \\ \left. + \int_{T_{\text{env}}}^{T_{\text{cal}}} (c_{p,\text{CaCO}_3} \frac{F_0}{F_{\text{R}}} + c_{p,\text{inert}} \frac{F_0 F_{\text{R,inert}}}{F_{\text{R}}}) dT \right. \\ \left. + (X_{\text{ave}} + \frac{F_0}{F_{\text{R}}}) \Delta H_{\text{CaCO}_3} \right\} \quad (6)$$

where E_{CO_2} is the CO_2 capture efficiency in the carbonator, as shown in Eq. (7) [12].

$$E_{\text{CO}_2} = \frac{(F_{\text{R}} + F_0) X_{\text{ave}}}{F_{\text{CO}_2}} \quad (7)$$

The following equation (as shown in Eq. (8)) proposed by Valverde [46] is used to describe the cyclic carbonation conversions under severe calcination conditions, as illustrated in Fig. 13. The

fitting parameters are summarized in Table 7.

$$X_N = X_r + \frac{X_1}{k(N-1) + \frac{X_1}{X_1 - X_r}} \quad (8)$$

According to Eq. (7), the CO₂ capture efficiencies under the severe calcination conditions with different circulation rates (i.e., F_R/F_{CO_2}) and supplement rates (i.e., F_0/F_R) are compared, as shown in Fig. 14. For limestone, carbide slag and CMT-5, E_{CO_2} increases with the increased F_0/F_R or F_R/F_{CO_2} . For the same F_R/F_{CO_2} , E_{CO_2} of CMT-5 is higher than those of carbide slag and limestone. For example, under the condition of $F_0/F_R=0.08$ and $F_R/F_{CO_2}=2$, E_{CO_2} of CMT-5 is 0.87, while E_{CO_2} of carbide slag and limestone only reach to 0.62 and 0.55, respectively. The F_0/F_R ratio of CMT-5 is only half as much as the value of carbide slag to reach E_{CO_2} of 90%. As a result, using CMT-5 in the calcium looping process is reasonable for achieving the goal of reducing the fresh sorbent makeup.

The relationship between the energy consumption in the calciner for capturing one mole of CO₂ and CO₂ capture efficiency is shown in Fig. 15. For the same ratio of F_0/F_R , $H_{cal}/F_{CO_2}E_{CO_2}$ declines at low E_{CO_2} level and increases at high E_{CO_2} level. The existence of minimum energy consumption shows the optimum operating conditions can be achieved. As shown in Fig. 14, E_{CO_2} increases with the increased ratio of F_0/F_R . However, the energy consumption in the calciner increases correspondingly, i.e., the energy for heating fresh sorbents to reach the calcination temperature. Moreover, E_{CO_2} slowly grows when F_0/F_R reaches to a certain degree and the degree of increase is greater in the energy consumption in the calciner. This attributes to the optimum F_0/F_R according to economics, which brings about the minimum energy consumption. It is obvious that $H_{cal}/F_{CO_2}E_{CO_2}$ of carbide slag and limestone are higher than that of CMT-5 in all cases and the largest

energy is consumed in the calciner using limestone. When F_R/F_{CO_2} ratio is 2 and E_{CO_2} is 0.9, $H_{cal}/F_{CO_2}E_{CO_2}$ for carbide slag and CMT-5 are 297.9 and 209.6 kJ/mol CO_2 , respectively, and thus the energy consumption of 88.3 kJ/mol CO_2 is saved when using CMT-5. The possible reason is that the carbonation reactivity of the sorbent increases and the sorbent makeup is depressed with the higher E_{CO_2} of CMT-5 than that of carbide slag. Therefore, the energy consumption in the calciner for raising the temperature of sorbents including unreacted CaO and fresh sorbents introduced into the calciner decreases.

The CaL process using the synthetic sorbent for post-combustion CO_2 capture from a coal-fired circulated fluidized bed (CFB) boiler is shown in Fig. 16. Carbide slag, alumina cement (mass ratio of calcined carbide slag to alumina cement = 95:5) and 1mol/L of glucose solution are added in a hydrothermal reactor at 180 °C for 6h. The obtained precipitate after the hydrothermal process is filtered, dried and sent into a pyrolyzer at 600 °C, and then fed into a pre-calciner at 600 °C under oxy-combustion to produce the synthetic sorbent. The obtained synthetic sorbent from the pre-calciner is stored in a sorbent tank. When CO_2 capture is required, the synthetic sorbent is fed into the CO_2 capture system including a calciner and a carbonator for cyclic CO_2 capture from the flue gas of a coal-fired CFB boiler.

4. Conclusions

An efficient calcium-based CO_2 sorbent has been developed using a carbon microsphere template route. Carbide slag, alumina cement and glucose served as low-cost calcium precursor, support and carbon source, respectively. Encouragingly, the synthetic sorbents show significantly better CO_2 capture performance than carbide slag. The synthetic sorbent with 5 wt.% alumina cement possesses the highest CO_2 capture capacity, which is 0.37 and 0.29 g/g after 20 cycles under the mild and severe calcination conditions, respectively. The choice of 1 mol/L of glucose is a relatively

economic and reasonable load for the carbon template. The optimal pre-calcination temperature is 600 °C. DFT calculations show that $\text{Ca}_{12}\text{Al}_{14}\text{O}_{33}$ can effectively retard the agglomeration of synthetic sorbents because Al sites on the $\text{Ca}_{12}\text{Al}_{14}\text{O}_{33}$ surface have strong interactions with the CaO cluster, which prevent the movement of the CaO clusters. The microstructure analysis confirms the hollow core-shell structure with higher porosity than carbide slag. Finally, the hollow core-shell model reveals that the typical meso-porous shell structure increases the exposed surface area of the synthetic sorbents and avoids the growth of unreacted CaO core to the greatest extent. Moreover, the physical separation effects of inert support, $\text{Ca}_{12}\text{Al}_{14}\text{O}_{33}$, further stabilize the sorbent reactivity, which attributes to the superior CO_2 capture performance of the synthetic sorbents. The F_0/F_R ratio of the synthetic sorbent with 5 wt.% alumina cement is only half as much as that of carbide slag to reach E_{CO_2} of 90%. When F_R/F_{CO_2} ratio is 2 and E_{CO_2} is 0.9, the energy consumption of 88.3 kJ/mol CO_2 is saved when using the synthetic sorbent with 5 wt.% alumina cement instead of carbide slag in the calciner. The novel calcium-based synthetic sorbent with hollow core-shell structure prepared from industrial solid waste seems particularly promising in the calcium looping process.

Acknowledgement

This work was supported by the Joint Foundation of National Natural Science Foundation of China and Shanxi Province for coal-based low carbon (U1510130) and Primary Research & Development Plan of Shandong Province, China (2016GSF117001).

Nomenclature

| | |
|-------|---|
| N | cycle number |
| C_N | CO_2 capture capacity of the sample after the N th calcination/carbonation cycle, g $(\text{CO}_2)/\text{g}$ (sorbent) |

| | |
|----------------------------|--|
| M_{CO_2} | molar mass of CO_2 , g/mol |
| M_{CaCO_3} | molar mass of CaCO_3 , g/mol |
| X_N | carbonation conversion of the sample after the N th cycle, mol/mol |
| m_0 | mass of the initial sample, g |
| m_N | mass of the sample after the N th carbonation, g |
| $m_{\text{cal},N}$ | mass of the sample after the N th calcination, g |
| b | CaO content in the initial sample, wt. % |
| T_{cal} | calcination temperature, K |
| T_{car} | carbonation temperature, K |
| T_{env} | environmental temperature, K |
| H_{cal} | energy consumption in the calciner, kJ/mol |
| F_0 | sorbent make-up flow rate, mol/s |
| F_R | flow rate of recycled sorbent, mol/s |
| $F_{R,\text{inert}}$ | flow rate of inert materials in the sorbent, mol/s |
| E_{CO_2} | CO_2 capture efficiency, % |
| F_{CO_2} | flow rate of CO_2 into the carbonator, mol/s |
| $c_{\rho, \text{CaO}}$ | heat capacity of CaO, J/(mol·K) |
| c_{ρ, CaCO_3} | heat capacity of CaCO_3 , J/(mol·K) |
| $c_{\rho, \text{inert}}$ | heat capacity of inert materials, J/(mol·K) |
| ΔH_{CaCO_3} | decomposing heat of CaCO_3 , kJ/mol |
| X_{ave} | average carbonation conversion of sorbents during carbonation process, mol/mol |
| X_r | residual conversion of sorbents after infinite calcination/carbonation cycles, mol/mol |

k decay coefficient of carbonation conversion

References

- [1] Liu T, Huffman T, Kulshreshtha S, McConkey B, Du Y, Green M, Geng X. Bioenergy production on marginal land in Canada: Potential, economic feasibility, and greenhouse gas emissions impacts. *Applied Energy* 2017;205:477-85.
- [2] Aminu MD, Nabavi SA, Rochelle CA, Manovic V. A review of developments in carbon dioxide storage. *Applied Energy* 2017;208:1389-419.
- [3] Erans M, Manovic V, Anthony EJ. Calcium looping sorbents for CO₂ capture. *Applied Energy* 2016;180:722-42.
- [4] Wang T, Yu W, Le Moullec Y, Liu F, Xiong Y, He H, Luo Z. Solvent regeneration by novel direct non-aqueous gas stripping process for post-combustion CO₂ capture. *Applied Energy* 2017;205:23-32.
- [5] Wang P, Guo Y, Zhao C, Yan J, Lu P. Biomass derived wood ash with amine modification for post-combustion CO₂ capture. *Applied Energy* 2017;201:34-44.
- [6] Valverde JM, Miranda-Pizarro J, Perejón A, Sánchez-Jiménez PE, Pérez-Maqueda LA. Calcium-looping performance of steel and blast furnace slags for thermochemical energy storage in concentrated solar power plants. *Journal of CO₂ Utilization*, 2017;22:143-154.
- [7] Tian S, Li K, Jiang J, Chen X, Yan F. CO₂ abatement from the iron and steel industry using a combined Ca-Fe chemical loop. *Applied Energy* 2016;170:345-52.
- [8] Benitez-Guerrero M, Valverde JM, Perejon A, Sanchez-Jimenez PE, Perez-Maqueda LA. Low-cost Ca-based composites synthesized by biotemplate method for thermochemical

- energy storage of concentrated solar power. *Applied Energy* 2018;210:108-16.
- [9] Jing J, Li T, Zhang X, Wang S, Feng J, Turmel WA, Li W. Enhanced CO₂ sorption performance of CaO/Ca₃A₁₂O₆ sorbents and its sintering-resistance mechanism. *Applied Energy* 2017;199:225-33.
- [10] Su C, Duan L, Donat F, Anthony EJ. From waste to high value utilization of spent bleaching clay in synthesizing high-performance calcium-based sorbent for CO₂ capture. *Applied Energy* 2018;210:117-26.
- [11] Li Y, Zhao C, Chen H, Ren Q, Duan L. CO₂ capture efficiency and energy requirement analysis of power plant using modified calcium-based sorbent looping cycle. *Energy* 2011;36:1590-8.
- [12] Zhang W, Li Y, He Z, Ma X, Song H. CO₂ capture by carbide slag calcined under high-concentration steam and energy requirement in calcium looping conditions. *Applied Energy* 2017;206:869-78.
- [13] Antzara A, Heracleous E, Lemonidou AA. Improving the stability of synthetic CaO-based CO₂ sorbents by structural promoters. *Applied Energy* 2015;156:331-43.
- [14] Blamey J, Zhao M, Manovic V, Anthony EJ, Dugwell DR, Fennell PS. A shrinking core model for steam hydration of CaO-based sorbents cycled for CO₂ capture. *Chemical Engineering Journal* 2016;291:298-305.
- [15] Valverde JM, Barea-López M, Perejón A, Sanchez-Jimenez PE, Pérez-Maqueda LA. Effect of thermal pretreatment and nanosilica addition on limestone performance at calcium-looping conditions for thermochemical energy storage of concentrated solar power. *Energy & Fuels* 2017;31:4226-36.

- [16] Chen H, Zhang P, Duan Y, Zhao C. CO₂ capture of calcium based sorbents developed by sol-gel technique in the presence of steam. *Chemical Engineering Journal* 2016;295:218-26.
- [17] Benitez-Guerrero M, Valverde JM, Sanchez-Jimenez PE, Perejon A, Perez-Maqueda LA. Calcium-Looping performance of mechanically modified Al₂O₃-CaO composites for energy storage and CO₂ capture. *Chemical Engineering Journal* 2018;334:2343-55.
- [18] Deng J, Li M, Wang Y. Biomass-derived carbon: synthesis and applications in energy storage and conversion. *Green Chemistry* 2016;18:4824-54.
- [19] Wu Z, Hao N, Xiao G, Liu L, Webley P, Zhao D. One-pot generation of mesoporous carbon supported nanocrystalline calcium oxides capable of efficient CO₂ capture over a wide range of temperatures. *Physical Chemistry Chemical Physics* 2011;13:2495-503.
- [20] Wang S, Zhao Q, Wei H, Wang JQ, Cho M, Cho HS, Terasaki O, Wan Y. Aggregation-free gold nanoparticles in ordered mesoporous carbons: toward highly active and stable heterogeneous catalysts. *Journal of the American Chemical Society* 2013;135:11849-60.
- [21] Wang J, Nie P, Ding B, Dong S, Hao X, Dou H, Zhang X. Biomass derived carbon for energy storage devices. *Journal of Materials Chemistry A* 2017;5:2411-28.
- [22] Wang K, Hu X, Zhao P, Yin Z. Natural dolomite modified with carbon coating for cyclic high-temperature CO₂ capture. *Applied Energy* 2016;165:14-21.
- [23] Zhao P, Sun J, Li Y, Wang K, Yin Z, Zhou Z, Su Z. Synthesis of efficient CaO sorbents for CO₂ capture using a simple organometallic calcium-based carbon template route. *Energy & Fuels* 2016;30:7543-50.
- [24] Broda M, Muller CR. Synthesis of highly efficient, Ca-based, Al₂O₃-stabilized, carbon gel-

- templated CO₂ sorbents. *Advanced Materials* 2012;24:3059-64.
- [25] Li Y, Liu H, Sun R, Wu S, Lu C. Thermal analysis of cyclic carbonation behavior of CaO derived from carbide slag at high temperature. *Journal of Thermal Analysis and Calorimetry* 2012;110:685-94.
- [26] Li Y, Su M, Xie X, Wu S, Liu C. CO₂ capture performance of synthetic sorbent prepared from carbide slag and aluminum nitrate hydrate by combustion synthesis. *Applied Energy* 2015;145:60-8.
- [27] Ma X, Li Y, Shi L, He Z, Wang Z. Fabrication and CO₂ capture performance of magnesia-stabilized carbide slag by by-product of biodiesel during calcium looping process. *Applied Energy* 2016;168:85-95.
- [28] Sun J, Liu W, Hu Y, Wu J, Li M, Yang X, Xu M. Enhanced performance of extruded-spheronized carbide slag pellets for high temperature CO₂ capture. *Chemical Engineering Journal* 2016;285:293-303.
- [29] Ma X, Li Y, Chi C, Zhang W, Shi J, Duan L. CO₂ capture performance of mesoporous synthetic sorbent fabricated using carbide slag under realistic calcium looping conditions. *Energy & Fuels* 2017;31:7299-308.
- [30] Burguete P, Corma A, Hitzl M, Modrego R, Ponce E, Renz M. Fuel and chemicals from wet lignocellulosic biomass waste streams by hydrothermal carbonization. *Green Chemistry* 2016;18:1051-60.
- [31] Mäkelä M, Yoshikawa K. Simulating hydrothermal treatment of sludge within a pulp and paper mill. *Applied Energy* 2016;173:177-83.
- [32] Luo C, Zheng Y, Xu Y, Ding H, Zheng C, Qin C, Feng B. Cyclic CO₂ capture characteristics

- of a pellet derived from sol-gel CaO powder with $\text{Ca}_{12}\text{Al}_{14}\text{O}_{33}$ support. Korean Journal of Chemical Engineering 2015;32:934-8.
- [33] Luo C, Zheng Y, Ding N, Zheng C. Enhanced cyclic stability of CO_2 adsorption capacity of CaO-based sorbents using La_2O_3 or $\text{Ca}_{12}\text{Al}_{14}\text{O}_{33}$ as additives. Korean Journal of Chemical Engineering 2011;28:1042-6.
- [34] Martavaltzi CS, Pampaka EP, Korkakaki ES, Lemonidou AA. Hydrogen production via steam reforming of methane with simultaneous CO_2 capture over CaO- $\text{Ca}_{12}\text{Al}_{14}\text{O}_{33}$. Energy & Fuels 2010;24:2589-95.
- [35] Shi J, Li Y, Zhang Q, Ma X, Duan L, Zhou X. CO_2 capture performance of a novel synthetic CaO/sepiolite sorbent at calcium looping conditions. Applied Energy 2017;203:412-21.
- [36] Grasa GS, Abanades JC. CO_2 capture capacity of CaO in long series of carbonation/calcination cycles. Industrial & Engineering Chemistry Research 2006;45:8846-51.
- [37] Hu Y, Liu W, Peng Y, Yang Y, Sun J, Chen H, Zhou Z, Xu M. One-step synthesis of highly efficient CaO-based CO_2 sorbent pellets via gel-casting technique. Fuel Processing Technology 2017;160:70-7.
- [38] Bartl H, Scheller T. Zur struktur des $12\text{CaO} \cdot 7\text{Al}_2\text{O}_3$. Neues Jahrb Mineral Monatsh 1970;35:547-52.
- [39] Ganguly R, Siruguri V, Gopalakrishnan I, Yakhmi J. Stability of the layered $\text{Sr}_3\text{Ti}_2\text{O}_7$ structure in $\text{La}_{1.2}(\text{Sr}_{1-x}\text{Ca}_x)_{1.8}\text{Mn}_2\text{O}_7$. Journal of Physics: Condensed Matter 2000;12:1683.
- [40] Tao X, Wang J, Liu C, Wang H, Yao H, Zheng G, Seh ZW, Cai Q, Li W, Zhou G. Balancing surface adsorption and diffusion of lithium-polysulfides on nonconductive oxides for

- lithium-sulfur battery design. *Nature communications* 2016;7:11203.
- [41] Galloway B, Padak B. Effect of flue gas components on the adsorption of sulfur oxides on CaO(100). *Fuel* 2017;197:541-50.
- [42] Tang H, Duan Y, Zhu C, Cai T, Li C, Cai L. Theoretical evaluation on selective adsorption characteristics of alkali metal-based sorbents for gaseous oxidized mercury. *Chemosphere* 2017;184:711-19.
- [43] Phromprasit J, Powell J, Wongsakulphasatch S, Kiatkittipong W, Bumroongsakulsawat P, Assabumrungrat S. Activity and stability performance of multifunctional catalyst (Ni/CaO and Ni/Ca₁₂Al₁₄O₃₃-CaO) for bio-hydrogen production from sorption enhanced biogas steam reforming. *International Journal of Hydrogen Energy* 2016;41:7318-31.
- [44] Liu L, Hong D, Guo X. A study of metals promoted CaO-based CO₂ sorbents for high temperature application by combining experimental and DFT calculations. *Journal of CO₂ Utilization* 2017;22:155-63.
- [45] Manovic V, Anthony EJ. Long-term behavior of CaO-based pellets supported by calcium aluminate cements in a long series of CO₂ capture cycles. *Industrial & Engineering Chemistry Research* 2009;48:8906-12.
- [46] Valverde JM. A model on the CaO multicyclic conversion in the Ca-looping process. *Chemical Engineering Journal* 2013;228:1195-206.
- [47] Li Y, Sun R, Liu C, Liu H, Lu C. CO₂ capture by carbide slag from chlor-alkali plant in calcination/carbonation cycles. *International Journal of Greenhouse Gas Control* 2012;9:117-23.

CO₂ capture performance of calcium-based synthetic sorbent with hollow core-shell structure under calcium looping conditions

Ma, Xiaotong

2018-05-15

Attribution-NonCommercial-NoDerivatives 4.0 International

Xiaotong Ma, Yingjie Li, Lunbo Duan, Edward Anthony, Hantao Liu, CO₂ capture performance of calcium-based synthetic sorbent with hollow core-shell structure under calcium looping conditions, *Applied Energy*, Volume 225, Issue September, 2018, Pages 402-412.

<https://doi.org/10.1016/j.apenergy.2018.05.008>

Downloaded from CERES Research Repository, Cranfield University